Nuclear Medicine in Pediatric Gastrointestinal Diseases

9

Angelina Cistaro and Michela Massollo

Contents

9.1 Ectopic Gastric Mucosa in Meckel's Diverticulum 150
9.2 Inflammatory Bowel Diseases 151
9.3 Appendicitis 153
9.4 Gastroesophageal Reflux and Esophageal Transit 156
9.4.1 Gastroesophageal Reflux 156
9.4.2 Esophageal Transit 156
9.4.3 Gastric Emptying 157
9.5 Hepatobiliary Scintigraphy 158
9.6 Hyperinsulinism 161
9.7 Protein-Losing Enteropathy 161
9.8 Colonic Transit 162
9.9 Gastrointestinal Bleeding 163
9.10 Hepatoblastoma 164
References 165

A. Cistaro (✉)
Positron Emission Tomography Centre, IRMET S.p.A., Euromedic Int., V.O. Vigliani 89, 10100, Turin, Italy

Chief of PET Pediatric AIMN Inter Group, Turin, Italy

Department of Nuclear Medicine, Institute of Cognitive Sciences and Technologies, National Research Council, Rome, Italy
e-mail: a.cistaro@irmet.com

M. Massollo
Department of Nuclear Medicine, Galliera Hospital, Mura delle Cappuccine 14, 10100, Genoa, Italy

© Springer International Publishing Switzerland 2016

L. Mansi et al. (eds.), *Clinical Nuclear Medicine in Pediatrics*,
DOI 10.1007/978-3-319-21371-2_9

9.1 Ectopic Gastric Mucosa in Meckel's Diverticulum

Gastrointestinal bleeding in pediatric patients can be suspected for the presence of Meckel's diverticulum (MD) that is caused by an incomplete closure of the omphalomesenteric duct and more frequently located in the ileum about 50–80 cm from the ileocecal valve. It occurs in 1–3 % of the population, more common in male patients. The ectopic gastric mucosa present in the diverticulum may result in mucosal damage and bleeding due to the production of acid and pepsin [1].

Scintigraphy with ^{99m}Tc-pertechnetate is an important and noninvasive test with a low radiation burden and it is easy to perform. In particular, it has a high accuracy for the detection of MD with ectopic gastric mucosa [2]. It is used to localize ectopic gastric mucosa in an MD [3, 4], due to the capacity of this tracer to avidly accumulate in gastric mucosa and then to reveal ectopic gastric mucosa in the diverticulum. The test represents still today the most accurate noninvasive technique for identifying ectopic gastric mucosa in Meckel's diverticulum, with high specificity and positive predictive value (close to 100 %) both in children and in adults [5, 6]. False-negative results may be due to barium enema, upper GI examination, recent in vivo RBC labeling, or again anatomic causes of error, such as small amount of gastric mucosa in Meckel's diverticulum, ischemia, or necrosis, or obscured by urinary tract activity (e.g., bladder) [3]. Moreover, false-positive result may be related to laxatives or endoscopy causing bowel irritation, urinary tract activity, lesions with increased blood pool, ulceration, inflammation, irritation, tumor, or intussusception.

Any type of patient preparation to performing the examination is not necessary, but it is important [3] to determine whether the patient has had recent in vivo RBC labeling in which all circulating RBCs were treated with stannous ion by intravenous administration of a "cold" pyrophosphate kit. If so, Meckel's scan may be compromised, because intravenous ^{99m}Tc-pertechnetate will label RBCs rather than concentrate in ectopic gastric mucosa. This may occur for days after the administration of stannous pyrophosphate. This is not a problem with in vitro labeling procedure.

The procedure requires an intravenous injection of 3.7 MBq/kg of body weight of ^{99m}Tc-pertechnetate and subsequent serial images of the abdomen, acquired for at least 30 min in the anterior view. A camera with large field of view is preferred and a collimator with a low-energy, all-purpose, parallel hole (photopeak, typically 20 % window at 140 keV; computer, 128 × 128 matrix, single- or two-byte mode). The left lateral decubitus position during the acquisition time can decrease small bowel activity arising from the stomach, increasing the diagnostic accuracy.

The images may be summed to make multiple sets of 10–15 min each, to facilitate interpretation of the data. Additional static images at the end of the dynamic series, as SPECT acquisition, can highly aid the identification of Meckel's diverticulum [7].

A positive scan demonstrates the appearance of focal activity in the ectopic gastric mucosa at the same time as in the normal gastric mucosa, although a small Meckel's diverticulum may appear later than the stomach. The most frequently anatomic position where it may be displayed is the right lower quadrant. The anatomic sites that most often can be misinterpreted to be the diverticulum are the kidneys

and the ureter or the bladder, in which there is an activity that, however, usually appears after that is seen in the normal gastric mucosa.

Some pharmacologic maneuvers have been reported to improve the detection of Meckel's diverticulum, for example, the use of pentagastrin, histamine H2 blockers, or glucagon [3]. Pentagastrin is a potent stimulator of gastric secretions and increases gastric mucosa uptake of pertechnetate and also stimulates the secretion of pertechnetate and GI motility, potentially reducing ectopic site activity. Histamine H2 blockers (cimetidine, ranitidine) block secretion from the cells and increase gastric mucosa uptake. Glucagon relaxes the smooth muscles of the GI tract, decreasing peristalsis. However studies with pentagastrin, histamine-H2 blockers, or glucagon are rarely performed [8], because pharmacologic pretreatment is not considered necessary for obtaining a high-quality Meckel's scan [3].

9.2 Inflammatory Bowel Diseases

Inflammatory bowel diseases (IBD) are diseases that often debut in late childhood or adolescence and include two different clinical entities causing chronic inflammation of the intestines, ulcerative colitis and Crohn's disease, that are chronic but characterized by alternating periods of relapse and remission [9].

Due to the continuous exacerbations of the disease, it is crucial to have a reliable and easily reproducible diagnostic test. However the endoscopic methods are invasive and require sedation, involving some risks, and often can only evaluate a limited portion of the colon. In addition, often there is a poor correlation between clinical symptoms and endoscopic [10–12] or histological findings, and, finally [13–15], the endoscopic findings cannot predict the response to the treatment [10–12, 14].

Autologous leukocytes labeled with ^{99m}Tc-hexamethylpropyleneamine oxime (HMPAO) is used to characterize active IBD [16–19]. The pathophysiologic basis of its use is correlated to the recruitment of the circulating leukocytes at the site of inflammation through a multistep process: adhesion to microvascular endothelium, transmigration through the vessel wall, and further migration in extravascular tissue and into the bowel lumen [20].

The diagnostic accuracy of ^{99m}Tc-HMPAO leukocyte scintigraphy in IBD is high, with sensitivity and specificity around 90 % [21]. It may be stated that a negative leukocyte scan virtually excludes the presence of active disease and the sensitivity of the method in untreated patients is high even in the early stages of disease, when radiologic or endoscopic findings are often normal or equivocal.

The labeling of leukocytes with ^{99m}Tc-HMPAO with 20–45 mL of venous blood has been described [16].

Two to 3 h after injection, and no later, an 8 min static anterior supine view of the abdomen and pelvis is obtained, followed by SPECT imaging to provide better localization of disease distribution [22].

A large field of view gamma camera with a low-energy, high-resolution collimator is usually preferred. Early imaging of the pelvis and abdomen is essential (bowel activity is seen in 20–30 % of children by 1 h and 2–6 % of adults by 3–4 h

postinjection). Regional images are obtained for at least 800,000 counts/large field of view of 5–10 min/view. Whole-body images should include the anterior and posterior head, chest, abdomen, pelvis, and extremities when clinically indicated. A limited study to evaluate a particular region of the body is acceptable in select cases. SPECT images of the chest, abdomen/pelvis, or spine may be helpful [23]. Accurate interpretation of labeled leukocyte scintigraphy requires knowledge of the normal and abnormal variants of leukocyte localization in the abdomen. Abnormal bowel localization may be seen by 15–30 min and usually increases in intensity over the next 2–3 h. The degree and extent of bowel disease are usually demonstrated by 1–2 h. Shifting patterns of bowel activity on later images usually indicate distal transit of labeled granulocytes or, at times, bleeding within the bowel lumen. False-positive results can occur from rapid small bowel transit of hepatobiliary secretion and focal accumulation of activity in the cecum, particularly if imaging is done after 1 h in children or 4 h in adults. Active gastrointestinal bleeding or swallowed cells can be mistaken for an inflammatory bowel process. Focal collections of inflamed peritoneal fluid or sites of focal bowel inflammation can be mistaken for abscess [23]. Volume-rendered images using the maximum-activity-projection or maximum-intensity-projection technique also are derived from the SPECT data in order to increase continuity of structures and facilitate comprehension of spatial relationships [24].

Although leukocyte imaging is useful, PET with 18F-FDG is becoming the new standard for nuclear medicine imaging in patients with IBD, based on the known potentiality of this tracer to localize the inflammatory lesions [9, 25, 26]. 18F-FDG has been proposed for imaging [31] infection/inflammation in part because it has been seen at sites of infection/inflammation during routine 18F-FDG imaging of cancer patients. Further studies showed that cells involved in infection and inflammation, especially neutrophils and the monocyte/macrophage family, are able to express high levels of glucose transporters, especially GLUT1 and GLUT3, and hexokinase activity [25, 32–35].

From limited experimental studies, it seems that the ability of the procedure to identify sites of inflammation and infection is related to the glycolytic activity of the cells involved in the inflammatory response. Many types of cells are involved in this process although no single cell was found specifically and consistently involved in all models. In addition, enhanced glucose consumption and subsequent 18F-FDG uptake can also be the result of a stress reaction of the affected cells in response to cell damage (metabolic flare) [36].

For this reasons, 18F-FDG PET and PET/CT have been proposed as noninvasive imaging methods to assess extent, location, and disease activity in adult and pediatric patients with IBD [9, 27, 28].

The diagnostic performance of 18F-FDG PET has proven to be excellent, with studies on pediatric patients where the average sensitivity was 98 % (higher than both endoscopy and abdominal ultrasound) and overall accuracy was comparable to the invasive procedure (83 % vs. 82 %) [25, 26]. Considering also that this technique avoids the long preparation times and the risks of radiolabeled autologous leukocytes, 18F-FDG PET may offer a definite clinical advantage for the patients [29].

Even if 18F-FDG PET/CT may not be able to replace conventional studies, this functional method may be useful when conventional studies cannot be performed or fail to be completed [30].

Patients must fast for at least 4 h before 18F-FDG imaging, during which time they should be encouraged to drink sufficient water to ensure hydration and promote diuresis. Necessary medications are allowed and must be recorded.

Because the effect of antibiotics on 18F-FDG uptake is unknown, it is useful to avoid such drugs, but no general recommendation on withdrawal can be stated. The patient should be advised to avoid strenuous physical exercise within 24 h before injection.

18F-FDG dose to obtain good imaging with a PET scanner operated in three-dimensional mode is optimized according to the EANM pediatric dosage card issued in 2008 [37].

With the current PET/CT scanners, the acquisition is performed in 3D whole-body mode, using steps of 1.5–3 min per bed position. Whole-body acquisition is usually defined as a field of view covering the head to mid thigh, starting in the pelvic area, when the bladder is empty.

In conclusion, 18F-FDG PET may be useful when endoscopic evaluation may not be feasible. In patients with an established diagnosis of IBD, 18F-FDG PET and PET/CT may provide information about disease activity, location, and extent within the intestinal tract, allowing early recognition of disease relapse and possible complications of the disease in association with clinical symptoms, physical exam, and laboratory data. 18F-FDG PET and PET/CT may guide decisions regarding the choice of therapy and may also allow the evaluation of efficacy of the medical therapy in IBD, because metabolic changes after the treatment (assessed by 18F-FDG PET) usually precede morphological changes assessed by conventional imaging methods (Figs. 9.1 and 9.2) [38, 39].

9.3 Appendicitis

Acute appendicitis is a surgical disease, particularly difficult to diagnosis in children. Delay in diagnosis is associated with morbidity from perforation, abscess, and peritonitis. It is therefore incumbent for the management of the pediatric patients with abdominal pain to correctly diagnose in order to treat patients appropriately.

In particular, in patients with abdominal pain and atypical or equivocal signs, symptoms, or laboratory tests, adjunctive imaging studies often are used to increase early diagnostic accuracy. Other than abdominal x-rays, ultrasound probably is the most commonly used adjunctive test for the patient with an atypical presentation. However, it has an accuracy of only 30 % in patients with early appendicitis because the appendix may not display the changes required for visualization [40].

^{99m}Tc-HMPAO-labeled leukocyte imaging is highly sensitive for detecting even small inflammatory processes in the abdomen because of high target-to-background ratio and early rapid uptake at sites of inflammation [41]. In fact, ^{99m}Tc-HMPAO is

Fig. 9.1 A 16-year-old boy with Crohn's disease. The maximum-intensity-projection 18F-FDG-PET image shows a diffuse and intense radiopharmaceutical uptake in the large bowel

an agent that complexes avidly with polymorphonuclear leukocytes, and it has a rapid uptake into areas of acute inflammation [42, 43].

An anterior image of the pelvis has to be acquired at 30–60 min postinjection, and it needs to be repeated at approximately 60 min intervals until either the scan showed abnormal uptake, indicating a positive scan, or remained negative until 3 h, at which time scanning was terminated.

There are a variety of abdominopelvic inflammatory processes that may be detected with ^{99m}Tc-WBC imaging, for example, inflammatory bowel disease,

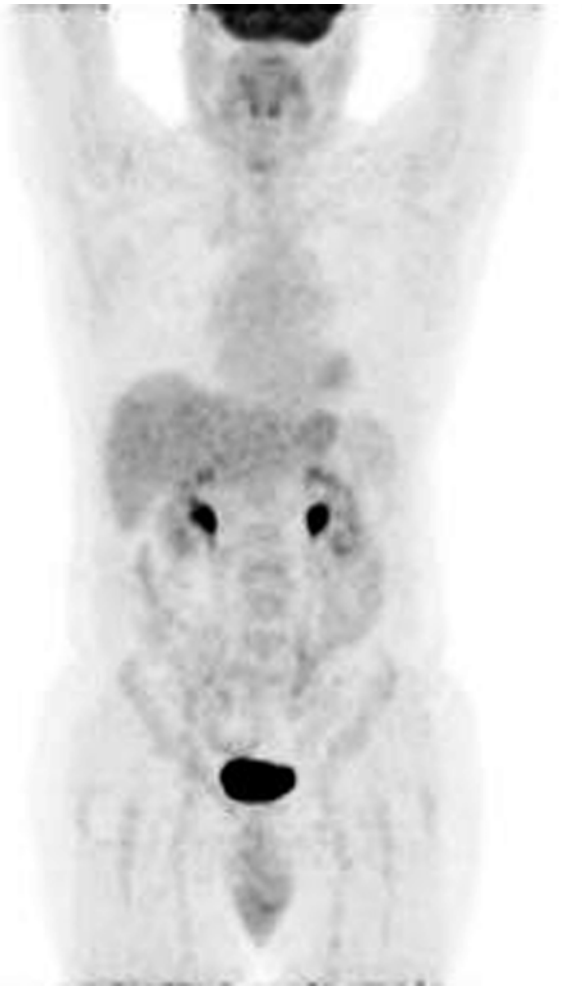

Fig. 9.2 The same patient in Fig. 9.1; 1 year later, posttreatment maximum-intensity-projection 18F-FDG-PET image shows a complete disappearance of any radiopharmaceutical uptake in the large bowel

abscess, and even bowel ischemia, and often differentiating between these conditions and appendicitis is not easy to obtain, and this results in a specificity of 85 % [16]. However, this issue can be obviated if the positive scans are interpreted in light of the overall clinical picture in order to consider ^{99m}Tc-HMPAO WBC imaging as an accurate, noninvasive test to exclude appendicitis in children with clinical suspicion of the disease but with anomalous presentation.

It is noted that inflammatory lesions show an avid uptake of 18F-FDG. The high resolution of PET, especially associated to CT or MR, together with the high concentration of 18F-FDG in inflammatory tissues, makes PET a potential useful tool for an earlier diagnosis of appendicitis and other abdominal inflammatory diseases. However, the use of 18F-FDG-PET in the detection of appendicitis is rare. More

often, it is an incidental finding of high 18F-FDG uptake in the right iliac fossa due to appendicitis during exams performed for malignancies. Familiarity with the normal pattern and physiologic variations of 18F-FDG distribution and with clinical data relevant to the patient can direct to a correct diagnosis, reducing a misleading differential diagnosis with tumors [44, 45].

9.4 Gastroesophageal Reflux and Esophageal Transit

Radionuclide studies for evaluating gastrointestinal transit in adults have been adapted for use in infants and children for assessing esophageal transit, gastroesophageal reflux, and gastric emptying.

9.4.1 Gastroesophageal Reflux

Gastroesophageal reflux, which is a condition characterized by the reflux of gastric and duodenal contents across the gastroesophageal junction into the esophagus, can occur in infants typically from 2 months of age. Typically, children can have symptom resolution by 18 months of age, and 30 % of them may have symptoms until the age of 4 years. The presence of gastroesophageal reflux may be related to severe complications, as strictures and pneumonia [46].

To provide information about esophageal and gastroesophageal function, nuclear medicine technique may be relevant with esophageal and gastroesophageal scintigraphy.

^{99m}Tc-sulfur colloid is often used for the assessment of gastroesophageal reflux in children, and the tracer should be added to two thirds of the feeding volume typical for the patient, with a dose of 0.1–1 mCi (3.7–37.0 MBq), in order to leave one third unlabeled to clear any remaining activity from the oropharynx and esophagus [47–49].

Gastroesophageal scintigraphy is best performed at the time of a usual feeding. Then, short-lasting 5 s anterior dynamic images are acquired for 60 min, and at the end, anterior and posterior static images of the thorax can be acquired to look for evidence of aspiration.

The dynamic images should be reviewed to recognize any episodes of reflux and regions of interest may be placed on the entire esophagus and on the upper esophagus to aid in the analysis of data and in order to demonstrate the number of episodes of reflux and level reached within the esophagus, and the clearance rate of reflux episodes may then be determined.

9.4.2 Esophageal Transit

Radionuclide-esophageal transit studies have been performed in infants, usually as part of the evaluation for reflux or in the evaluation of patients with esophageal

motility disorders such as achalasia, diffuse esophageal spasm, nutcracker esophagus, tracheoesophageal fistula, Down syndrome, esophagitis, systemic sclerosis, and diabetes mellitus.

Other diagnostic methods, as esophageal manometry, contrast radiography, and endoscopy, may be used to assess esophageal peristalsis, anatomical lesions, and mucosal lesions, but the advantages of esophageal scintigraphy include its noninvasive nature, quantifiability, and low radiation burden. Its clinical application has been suggested to be useful when the other procedures are unavailable or not tolerated by the patient or when the results are equivocal [49–55].

A 10 mL bolus of water or milk labeled with 150 μCi (5.55 MBq) of ^{99m}Tc-sulfur colloid is administered to the patient in the supine position. Posterior images at 0.4 s intervals for 150 frames are acquired, including the mouth and stomach, in the camera field of view. A radioactive bolus is placed in the mouth and swallowed on command followed by a dry swallow 30 s later. Abnormal studies may be repeated in the upright position to determine the effect of gravity.

Image analysis is performed by the evaluation of time activity curves derived from regions of interest placed on the upper, middle, and lower thirds of the esophagus and on the stomach. This procedure may demonstrate abnormal esophageal transit in pathologic states and may also visualize esophageal transit condensing dynamic images.

Usually, the normal transit time through the esophagus is typically less than 10 s. Esophageal transit ranges from 3.4 ± 1 s for infants to 4.6 ± 1.9 s for patients 8–16 years of age. Gastroesophageal reflux and esophagitis are associated with prolonged transit times [56].

9.4.3 Gastric Emptying

Patients with abnormal gastric emptying may present nausea, vomiting, abdominal discomfort, early satiety, diarrhea, and “dumping.”

The correct assessment of gastric emptying helps to guide treatment decisions, particularly in the neurologically impaired children that frequently demonstrate symptomatic delayed gastrointestinal motility.

Furthermore, delayed gastric emptying may be secondary to several pathological conditions, as pyloric or duodenal stenosis, acidosis, hypothyroidism, autonomic neuropathy associated with diabetes mellitus, central nervous system disease, systemic lupus erythematosus, dermatomyositis/polymyositis, infection, and many others.

The rate of gastric emptying assessed scintigraphically has been shown to depend on the type of meal used: liquids typically empty faster than solids.

In infants, a milk or formula feeding is usually administered and the type of milk and volume fed should be standardized according to patient size. However, many of the patients studied have feeding difficulties and in these cases is difficult to standardize the volume fed.

The dose of ^{99m}Tc-sulfur colloid added to the milk depends on whether gastric emptying is performed in conjunction with the reflux study.

If only the rate of emptying is of interest, this dose can be decreased to 100 μCi (3.7 MBq).

In older children, solid gastric emptying may be performed by having the patient eat an egg sandwich containing ^{99m}Tc-sulfur colloid (250–300 μCi). The meal should be scaled according to patient size (where adults are given 4 eggs and 50 mL of water). Thirty second anterior images are acquired every 10 min. Between images, the patient should sit upright. Images are acquired until 120 min.

A region of interest is drawn around the stomach. Activity from the bowel should not be included in the region of interest.

The range for normal gastric emptying has been difficult to establish in children for ethical reasons. Furthermore, the test meals have not been standardized. In general, laboratories have to decide on the values to be used based on their own experience. A study performed several years ago in children thought to be normal retrospectively shown, for milk, a residual of 36–68 % at 60 min and 42–56 % in a small number of older children [57].

In another report using dextrose as the test meal, the 60 min residual was 27–81 % in children under 2 years of age and 11–47 % in older children. This age-related difference in emptying rate has been observed by others, although the composition of the meal may also play a role [58].

9.5 Hepatobiliary Scintigraphy

Hepatobiliary scintigraphy is useful in the assessment of patients with right upper quadrant pain, in particular if there is the suspicion of acute cholecystitis. Cholecystitis is less common in children than in adults, but its incidence in pediatric patients has probably been underestimated [59, 60].

It is possible to recognize two types of cholecystitis: acute calculous cholecystitis, which occurs when the cystic duct becomes obstructed by gallstones leading to gallbladder distension and edema, and acalculous cholecystitis, which can occur in prolonged illness, sepsis, or trauma.

Both of these conditions may be associated with inflammation and edema and consequently with blood flow impairment and bacterial infection advancement.

Typically, the most common symptoms in children are abdominal pain localized in the right upper quadrant or epigastric region. Other symptoms include nausea, vomiting, anorexia, and fever for several days.

The most common clinical signs are represented by a right upper quadrant tenderness, jaundice, and enlarged and palpable gallbladder. Regarding the laboratory tests, leukocytosis is a common finding [61–63]. In the diagnosis of cholecystitis, ultrasound is basic in the evaluation of the biliary tract and detecting gallstones; however, its diagnostic accuracy presents a substantial margin of error. In a recent systematic review of different imaging modalities in patients with suspected acute cholecystitis [64], hepatobiliary scintigraphy is the most accurate diagnostic

imaging modality for acute cholecystitis, with a sensitivity and specificity for hepatobiliary scintigraphy of 96 % and 90 %, respectively. The sensitivity of hepatobiliary scintigraphy results significantly higher than ultrasound (81 %).

^{99m}Tc-disofenin or ^{99m}Tc-mebrofenin is administered intravenously, with a dose for infants and children of 1.85 MBq/kg (0.05 mCi/kg). Mebrofenin is always preferred in jaundiced infants with hyperbilirubinemia, with a minimum administered activity of 37 MBq (1.0 mCi), as up to 24 h delayed images are often required. The patient should be fasting for 4 h prior to the test. Immediately after the injection, dynamic imaging is acquired for 60 min (0.5–1 min/frame) in anterior projects using preferably a high-resolution collimator and 128×128 matrix. Additional views such as right lateral and left or right anterior oblique may be performed, if required. When acute cholecystitis is suspected and the gallbladder is not seen within 60 min, delayed images for up to 4 h should be obtained [65].

In adult patients, acute cholecystitis is associated with non-visualization of the gallbladder on hepatobiliary scintigraphy, and the visualization of gallbladder activity excludes the diagnosis of acute cholecystitis with high accuracy. However, in children, the presence of cholecystitis is not entirely excluded if there is gallbladder visualization, because this is possible in acalculous cholecystitis [46]. After 60 min images, if the gallbladder is visualized, it is possible to perform additional dynamic imaging for 60 min following infusion of 0.02 μg/kg sincalide, a synthetic C-terminal octapeptide of cholecystokinin. Poor contraction and emptying of the gallbladder following sincalide may occur in partial cystic duct obstruction, acalculous cholecystitis, or chronic cholecystitis.

Hepatobiliary scintigraphy in children can also be used for the evaluation of choledochal cyst and biliary leak. Biliary atresia is characterized by obliteration or discontinuity of the extrahepatic biliary system, resulting in obstruction of bile flow [66]. The disorder represents the most common surgically treatable cause of cholestasis encountered during the newborn period. If not surgically corrected, secondary biliary cirrhosis invariably results. In infants, hepatobiliary scintigraphy is used to differentiate biliary atresia from hepatocellular disease [67]. The disorder, if not surgically corrected, results in secondary biliary cirrhosis. Thus early diagnosis of biliary atresia remains imperative, and the gold standard within the diagnostic modalities is liver biopsy and/or intraoperative cholangiogram. Studies have demonstrated 100 % sensitivity of ^{99m}Tc-mebrofenin hepatobiliary scintigraphy (HIDA scan) for picking up biliary atresia, and its specificity has been reported to range from 88.6 to 92 % [68, 69].

The premedication with phenobarbital or ursodeoxycholic acid before hepatobiliary scintigraphy may increase bile secretion and improves the diagnostic differentiation between biliary atresia and neonatal hepatitis [65]. The administered activity for infants and children is 1.8 MBq/kg (0.05 mCi/kg), with a minimum administered activity of 18.5 MBq (0.5 mCi). Mebrofenin is always preferred in neonates with hyperbilirubinemia, with a minimum administered activity of 37 MBq (1.0 mCi), as up to 24 h delayed images are often necessary [67].

For the image acquisition [67], a large-field-of-view γ-camera equipped with a low-energy all-purpose or high-resolution collimator is recommended. Whenever

possible, continuous (dynamic) computer acquisition (usually in the anterior or left anterior oblique view) should be performed (1 frame/min). The image matrix of 128 by 128 is optimal on a standard large-field-of-view camera. In pediatric patients, an appropriate electronic acquisition zoom should be used. Initial images are usually acquired dynamically, starting at injection and continuing for 60 min. When visualization of the gallbladder is the end point of the study, it can be stopped earlier when activity is seen in the gallbladder. Additional views (e.g., right lateral, left or right anterior oblique) may be obtained as needed to clarify anatomy. To resolve concern about common bile duct obstruction (highly unlikely in the presence of gallbladder visualization), demonstration of tracer activity in the small bowel may need to be pursued.

The digital data can be reformatted to 4 to 6 min images for filming or digital display. Cinematic display of the data may reveal additional information not readily apparent on reformatted display. Image intensity scaling should be study relative rather than individual frame relative. The former allows for appreciation of activity changes over the duration of the study.

If there is visualization of the biliary drainage of the radiotracer into the bowel, scintigraphy can exclude the presence of biliary atresia. If no bowel activity is detected up to 24 h and liver uptake is normal, the diagnosis of biliary atresia is suspected [46, 67]. If the patient is being studied for a biliary leak, 2 to 4 h delayed imaging (or longer delays in some cases) and patient-positioning maneuvers (e.g., decubitus views) may be helpful. Any drainage bags should be included in the field of view if the biliary origin of a leak or fistula is in question. In patients with a suspected leak, it may be helpful to acquire simultaneous right lateral or other views on a multihead camera.

However, normal liver uptake of tracer with no excretion up to 24 h can occur in severe cases of neonatal hepatitis, Alagille syndrome, dehydration, sepsis, TPN cholestasis, and bile plug syndrome in cystic fibrosis. Neonatal hepatitis typically demonstrates reduced hepatocyte uptake and delayed hepatobiliary transit of tracer into the bowel [46]. Failure of tracer to enter the gut is consistent with biliary atresia but can also be caused by hepatocellular disease or immature intrahepatic transport mechanisms. Renal or urinary excretion of the tracer (especially in a diaper) may be confused with bowel activity and is a potential source of erroneous interpretation [67].

An interesting application of 18F-FDG PET in this setting is its use in children with biliary cirrhosis and fever of unknown origin (FUO) on the waiting list for liver transplantation. Infection imaging with FDG-PET relies on the fact that granulocytes and mononuclear cells use glucose as an energy source specifically during their metabolic burst upon activation by triggers. The advantages of FDG-PET are early imaging after injection, higher resolution and higher target-to-background ratio, sensitivity to chronic low-grade infections, and high interobserver agreement [70].

Systemic infections are considered to be contraindications for liver transplantation; however, hepatic infections are frequently only cured by the removal of the infected organ during transplantation. Therefore the information obtained by FDG-PET imaging to identify intrahepatic infections may be crucial for the management of patients with FUO awaiting liver transplantation [71].

9.6 Hyperinsulinism

Congenital hyperinsulinism (CHI) is a rare disease of hypoglycemia due to dysregulated and excessive insulin secretion, with an incidence of severe cases estimated at 1:50,000 and the incidence rising in consanguineous populations [72, 73].

In infants, the treatment of congenital hyperinsulinism is required to prevent possible neurologic complications. Forty percent of cases of hyperinsulinism in children results from pathologic adenomatous pancreatic β-cells. Diffuse hyperinsulinism involves the whole pancreas with enlarged abnormal β-cell nuclei. Ten percent of cases of infantile hyperinsulinism are atypical and fit neither classification. Focal hyperinsulinism is cured by resection of the adenoma, whereas diffuse pancreatic involvement may be treated with subtotal pancreatectomy. [74, 75].

Positron emission tomography (PET) using 6-L-(18)F-fluorodihydroxyphenylalanine ((18)F-DOPA) may be useful for classifying pancreatic involvement in infantile hyperinsulinism as focal or diffuse and can be used preoperatively to identify the two forms of infantile hyperinsulinism, differentiating between patients who should receive curative focal pancreatic resection and those who should receive medical management [76, 77]. (18)F-DOPA is a radioactive isotope of L-dihydroxyphenylalanine (L-DOPA), an intermediate in the catecholamine synthesis pathway. L-DOPA is avidly taken up by neuroendocrine cells, including CHIb-cells, while uptake is minimal in the normal pancreas. It is not understood why CHI pancreatic tissues exhibit more a differential uptake and retention pattern than normal tissue, particularly as CHI is not apparently linked with altered catecholamine metabolism.

Initial observations showed a high sensitivity (88–94 %) and specificity (100 %) of (18)F-DOPA PET imaging in differentiating focal from diffuse CHI [78, 79] which was further enhanced by the concurrent use of CT angiography using iodine-based dyes. The latter is useful to localize the site of the lesion, in relation to anatomical structures, which is particularly useful at the time of focal lesionectomy. Although meta-analyses of (18)F-DOPA PET imaging studies indicate good diagnostic performance [80, 81], recent studies have suggested that the predictive value of scanning may not be as accurate as initially estimated [82, 83].

9.7 Protein-Losing Enteropathy

Protein-losing enteropathy can be the result of primary intestinal lymphangiectasia or secondary intestinal lymphangiectasia in association with cardiac diseases or obstructed lymphatics. Abnormal or inflamed mucosal surface secondary to intestinal inflammation/infection and immunologic, inflammatory, and vasculitic disorders can also cause enteric protein loss [84].

This pathophysiologic condition generally results from an abnormal mucosal permeability, desquamation, inflammation, or back pressure in the intestinal lymphatic network [85].

The protein loss is nonselective and includes plasma proteins such as albumin, globulins, and transferrin. Radiolabeled proteins that have been used for determining enteric protein loss include 131I-albumin, 51Cr-albumin, and 67Cu-ceruloplasmin [84].

^{99m}Tc-human serum albumin (HSA) has been successful in localizing the site of enteric protein loss in adults [86–92]; however, the literature is lacking concerning pediatric patients [93–95].

A study performed on children [96] reported that the scan has a higher sensitivity in patients with lower albumin and total protein values, presumably reflecting a higher rate of protein loss; they submitted all patients to an anterior abdominal scintigraphy after the intravenous injection of freshly prepared ^{99m}Tc-HAS. The administered age-adjusted doses were 185–503 MBq based on an adult dose of 740 MBq. They acquired dynamic images every minute for 1 h, using an all-purpose collimator and a large-field-of-view γ-camera. Additional delayed images were obtained at 2–6 h in most patients and 24 h in a few patients.

They found enteric ^{99m}Tc-HSA uptake in 67 % of the children, suggesting the site of protein loss. The location of the uptake was most likely in the small bowel in 91 % of the early images and in 27 % of the delayed images. Colonic activity was noted in 72 % of the delayed images, most likely representing transit of activity rather than a second site of protein loss.

9.8 Colonic Transit

Two different types of chronic functional constipation have been identified in children based on colonic transit time measurement: a more generalized and severe form known as slow transit constipation and a segmental type known as functional fecal retention [97].

Both entities present with similar symptomatology but involve different pathophysiological mechanisms and require different treatment strategies.

It has been shown that children thus classified respond to different treatment strategies. Only a small proportion of cases require surgical intervention such as appendicostomy, colostomy, or colonic resection [99–101]. The different types of abnormal colonic transit can be identified using radiopaque markers: slow transit (pancolonic or globalized delay), normal transit, and functional fecal retention (outlet obstruction or distal obstruction) [98]. Colonic transit scintigraphy can aid in the identification and therapeutic decision-making in patients with functional fecal retention, the most common cause of chronic constipation in children [102].

This method has been used to determine colonic transit in adults with chronic constipation, and the reported advantages, compared with radiopaque marker studies, include a low radiation dose and the acquisition of multiple images allowing estimates of gastric, small bowel, and segmental colonic transit to be made [103, 104].

Intake of laxatives has to be stopped 5 days before the transit studies, and fasting is required for 4 h before the start of the test. The radiopharmaceutical ^{99m}Tc-calcium phytate colloid, suspended in 20 mL of milk, can be administered by mouth. The dose is determined according to each patient's weight and is based

on an adult dose of 250 MBq. Anterior and posterior view images are obtained immediately after ingestion and during the subsequent 2 h to estimate gastric emptying. Three categories of colonic transit could be readily distinguished by visual assessment of the acquired images. In studies considered to demonstrate normal transit, the tracer reached the cecum by 6 h, passed through the colon, and was largely excreted by 48 h. Slow transit was identified when the tracer reached the cecum at 6 h, but most radioactivity was retained in the proximal colon and transverse colon at 24, 30, and 48 h. Patients in whom the tracer reached the rectosigmoid by 24–30 h but was not passed at 48 h were appreciated. This pattern was defined as consistent with functional fecal retention or outlet obstruction.

9.9 Gastrointestinal Bleeding

Gastrointestinal (GI) bleeding is often encountered in daily clinical settings. Dramatic advances in endoscopic technology in recent years have facilitated diagnosis and treatment of bleeding from the esophagus, stomach, and duodenum, as well as most cases of bleeding from the large intestine. Although it is now possible to observe the small intestine using video capsule endoscopy and double-balloon enteroscopy [105], diagnosing the source of GI bleeding and providing treatment remain the challenges in some patients [106].

GI bleeding scintigraphy is a noninvasive examination that enables detection with a bleeding rate as low as 0.1 mL/min [107]. In children, while most gastrointestinal bleeding may not be life threatening, it is necessary to determine the source, degree, and possible cause of the bleeding and to distinguish minor from major bleeding [108]. In the stable child with occult bleeding, management is geared toward making the diagnosis and excluding more serious conditions. Investigations are directed by the history and physical examination, but most diagnostic tests can be performed on an outpatient basis [109].

^{99m}Tc-red blood cell (RBC) scintigraphy generally is useful for assessing GI bleeding in patients. Meckel's diverticula also may be identified through this technique, although other causes of bleeding may include intussusception, IBD, Henoch-Schonlein purpura, gastritis, duodenitis, Mallory-Weiss tear, infectious enterocolitis, allergic enterocolitis, midgut volvulus, polyps, tumors, vascular malformations, enteric duplication cysts, nodular lymphoid hyperplasia, hemolytic uremic syndrome, and foreign body and trauma [110].

The main advantage of the use of ^{99m}Tc-RBCs is the possibility of visualization of GI bleeding over the course of several hours. Bleeding rates as low as 0.1–0.4 mL/min may be detected. Large bowel endoscopy of actively bleeding patients has a low diagnostic yield and is potentially harmful to the patient, and the small bowel is not successfully visualized endoscopically. Angiography typically localizes bleeding when the rate is greater than 1 mL/min. However, for bleeding to be identified, it should occur during the 20 to 30 s time interval during which contrast is administered. Scintigraphy permits the visualization of the entire GI tract.

Labeling of RBCs is most efficient by the in vitro method (98 %) as compared with the in vivo (70 %) and modified in vivo (90–95 %) methods. The disadvantage of lower labeling efficiencies is the possibility of secretion of free pertechnetate within the gastric mucosa into the duodenum and also the excretion of free pertechnetate into the urinary collecting system increasing the likelihood of false-positive studies.

Positive studies demonstrate tracer activity outside of normal vascular structures with antegrade or retrograde motion of tracer through bowel. The motion is best detected on cinematic display and may occur very rapidly. Small bowel bleeding may be distinguished from a colonic source by the demonstration of rapid distal progression through a series of multiple small, centrally located, curvilinear segments on cinematic display of the abdomen. Large bowel bleeding has a more elongated pattern with peripheral location within the abdomen compared with bleeding within small bowel. Stationary activity is more likely to represent a vascular abnormality and urinary or penile activity. In rare cases, a stationary site may represent adherent blood clot to the bowel wall.

^{99m}Tc-sulfur colloid also has been used in the assessment of GI bleeding. It has the advantage of detecting rates as low as 0.05–0.1 mL/min through the achievement of a high bleeding to background ratio. Its disadvantages include a short duration of imaging time to localize bleeding of approximately 20 min and limited interpretation of potential bleeding sites in proximity to the liver and spleen as these structures accumulate ^{99m}Tc-sulfur colloid during the test.

Both ^{99m}Tc-RBC scintigraphy and ^{99m}Tc-sulfur colloid scintigraphy detect sources of venous and arterial GI bleeding, whereas contrast angiography only detects arterial sources [111–114].

9.10 Hepatoblastoma

Hepatoblastoma (HB) is the most common primary malignant hepatic tumor in childhood [115, 116]. According to the histology, HB can be in pure epithelial and mixed type, the latter being formed by epithelial and mesenchymal components. The clinical onset is characterized by an abdominal mass, while in the advanced disease, anorexia and weight loss can also be present. Ninety percent of cases present increased level of serum alpha-fetoprotein (α-FP).

At present, complete resection is possible in more than 50 % of cases, and preoperative chemotherapy has been successfully used in converting unresectable to resectable tumors [117–119]. Liver transplantation has been proposed as an option in patients with unresectable tumors.

The follow-up is based on the association between laboratory analysis and imaging.

In particular, although a rising level of serum α-FP is generally associated with tumor recurrence, most protocols require additional imaging follow-up in order to localize neoplastic lesions, as US, CT, or RM [120–122]. However, early detection of recurrent hepatoblastoma is not always possible with conventional imaging methods such as CT and MRI.

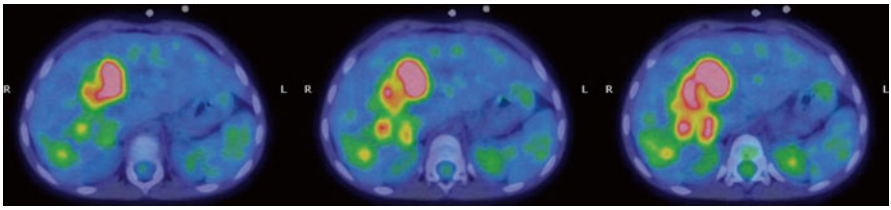

Fig. 9.3 A 4-year-old boy affected by hepatoblastoma. PET evaluation was performed to establish liver transplantation eligibility. Axial PET/CT fusion images show 18F-FDG-avid lesions in the liver

A further dimension of information based on the regional biochemical and physiological abnormalities can be provided by positron emission tomography (PET) using F18-fluorodeoxyglucose (FDG), which has been successfully used for the last two decades in localizing primary and metastatic tumors in adults [123–125]. It is known that 18F-FDG uptake in tumors is proportional to the metabolic rate of viable tumor cells, which have an increased demand for glucose than normal tissue. It has already been proven that hepatoblastoma cells have demonstrated prominent glycogen granules in the cytoplasm [126, 127], and this fact may suggest active accumulation of glucose and its transformation and accumulation in glycogen granules [128] and consequently can explain the uptake of 18F-FDG.

The whole-body PET/CT scan has to be performed as a standard examination, following the guidelines for the administered dose and for the acquisition parameters of the PET imaging in pediatrics.

18F-FDG PET/CT could provide incremental diagnostic value in the initial evaluation of patients affected by hepatoblastoma, helping to detect additional metastatic sites at diagnosis.

However, 18F-FDG PET/CT has no established role in the initial diagnosis of hepatoblastoma [129], but it is helpful in detecting early recurrence [130], and few studies have evaluated its role in follow-up and restaging of patients after chemotherapy and surgery [131–135].

Since experience is so far limited in the literature [136], multicenter and prospective studies are warranted to suggest the introduction of 18F-FDG-PET/CT in the routine imaging workup for hepatoblastoma staging and in case of suspicion of relapse (Fig. 9.3).

References

1. Maurer AH, Parkman HP (2006) Update on gastrointestinal scintigraphy. Semin Nucl Med 36:110–118
2. Jung Hee Rho et al (2013) Clinical features of symptomatic Meckel's diverticulum in children: comparison of scintigraphic and non-scintigraphic diagnosis. PGHN 16:41–48
3. Ford PV et al (1999) Procedure guideline for gastrointestinal bleeding and Meckel's diverticulum scintigraphy. Society of Nuclear Medicine. J Nucl Med 40:1226–1232
4. Sfakianakis GN, Conway JJ (1981) Detection of ectopic gastric mucosa in Meckel's diverticulum and in other aberrations of scintigraphy: I: pathophysiology and 10 year clinical experience. J Nucl Med 22:647–654

5. Sfakianakis GN, Haase GM (1982) Abdominal scintigraphy for ectopic gastric mucosa: a retrospective analysis of 143 studies. AJR Am J Roentgenol 138:7–12
6. Kong MS et al (1993) Technetium-99m pertechnetate scan for ectopic gastric mucosa in children with gastrointestinal bleeding. J Formos Med Assoc 92:717–720
7. Connolly LP et al (1998) Meckel's diverticulum: demonstration of heterotopic gastric mucosa with technetium-99m-pertechnetate SPECT. J Nucl Med 39:1458–1460
8. Brown ML (1995) Gastrointestinal bleeding. In: Wagner HN, Szabo Z, Buchanan JW (eds) Principles of nuclear medicine, 2nd edn. Saunders, Philadelphia, pp 929–934
9. Treglia G et al (2012) Diagnostic performance of Fluorine-18 Fluorodeoxyglucose positron emission tomography in patients with chronic inflammatory bowel disease: a systematic review and a meta-analysis. J Crohn Colitis 7:345–354
10. Daum F et al (1989) Does proctosigmoiditis in inflammatory bowel disease presage the imminent onset of symptoms? J Pediatr Gastroenterol Nutr 8:339–342
11. Modigliani R et al (1990) Clinical, biological, and endoscopic picture of attacks of Crohn's disease. Evolution on prednisolone. Groupe d'Etude Therapeutique des Affections Inflammatoires Digestives. Gastroenterology 98:811–818
12. Modigliani R (1990) Endoscopic severity index for Crohn's disease. Gastrointest Endosc 36:637
13. Gomes P et al (1986) Relationship between disease activity indices and colonoscopic findings in patients with colonic inflammatory bowel disease. Gut 27:92–95
14. Landi B et al (1992) Endoscopic monitoring of Crohn's disease treatment: A prospective, randomized clinical trial. The Groupe d'Etudes Therapeutiques des Affections Inflammatoires Digestives. Gastroenterology 102:1647–1653
15. Pera A et al (1987) Colonoscopy in inflammatory bowel disease. Diagnostic accuracy and proposal of an endoscopic score. Gastroenterology 92:181–185
16. Charron M et al (1994) Detection of inflammatory bowel disease in pediatric patients with technetium-99m-HMPAO-labeled leukocytes. J Nucl Med 35:451–455
17. Li DJ et al (1994) Can 99Tcm HMPAO leucocyte scintigraphy distinguish between Crohn's disease and ulcerative colitis? Br J Radiol 67:472–477
18. Datz FL et al (1997) Procedure guideline for technetium-99m- HMPAO-labeled leukocyte scintigraphy for suspected infection/inflammation. Society of Nuclear Medicine. J Nucl Med 38:987–990
19. Martin-Comin J, Prats E (1999) Clinical applications of radiolabeled blood elements in inflammatory bowel disease. Q J Nucl Med 43:74–82
20. Muller WA (2002) Leukocyte-endothelial cell interactions in the inflammatory response. Lab Invest 82:521–533
21. Annovazzi A et al (2005) Nuclear medicine imaging of inflammatory/infective disorders of the abdomen. Nucl Med Commun 26:657–664
22. Charron M et al (1999) Pediatric inflammatory bowel disease: assessment with scintigraphy with 99mTc white blood cells. Radiology 212:507–513
23. Society of Nuclear Medicine Procedure Guideline for 99mTc-Exametazime (HMPAO)-Labeled Leukocyte Scintigraphy for Suspected Infection/Inflammation Version 3.0, approved June 2, 2004
24. Wallis JW, Miller TR (1990) Volume rendering in three-dimensional display of SPECT images [see comments]. J Nucl Med 31:1421–1428
25. Yamada S et al (1995) High accumulation of fluorine-18 fluorodeoxyglucose in turpentine-induced inflammatory tissue. J Nucl Med 36:1301–1306
26. Love C et al (2005) FDG PET of infection and inflammation. Radiographics 25:1357–1368
27. Loffler M et al (2006) High diagnostic value of 18F-FDG-PET in pediatric patients with chronic inflammatory bowel disease. Ann N Y Acad Sci 1072:379–385
28. Cistaro A et al (2012) The role of positron emission tomography in inflammatory bowel disease. Eur J Inflam 3:251–256
29. Neurath MF et al (2002) Noninvasive assessment of Crohn's disease activity: a comparison of 18F-fluorodeoxyglucose positron emission tomography, hydromagnetic resonance imaging, and granulocyte scintigraphy with labeled antibodies. Am J Gastroenterol 97:1978–1985

30. Däbritz J et al (2011) Noninvasive assessment of pediatric inflammatory bowel disease with 18F-fluorodeoxyglucose-positron emission tomography and computed tomography. Eur J Gastroenterol Hepatol 23:81–89
31. Jamar F et al (2013) EANM/SNMMI guideline for 18F-FDG use in inflammation and infection. J Nucl Med 54:647–658
32. Mochizuki T et al (2001) FDG uptake and glucose transporter subtype expressions in experimental tumor and inflammation models. J Nucl Med 42:1551–1555
33. Kubota R et al (1992) Intratumoral distribution of fluorine-18-fluorodeoxyglucose in vivo: high accumulation in macrophages and granulation tissues studied by microautoradiography. J Nucl Med 33:1972–1980
34. Gamelli RL et al (1996) Augmentations of glucose uptake and glucose transporter-1 in macrophages following thermal injury and sepsis in mice. J Leukoc Biol 59:639–647
35. Fukuzumi M et al (1996) Endotoxin-induced enhancement of glucose influx into murine peritoneal macrophages via GLUT1. Infect Immun 64:108–112
36. Mortimer JE et al (2001) Metabolic flare: indicator of hormone responsiveness in advanced breast cancer. J Clin Oncol 19:2797–2803
37. www.eanm.org/docs/dosagecard.pdf
38. Treglia G et al (2013) Diagnostic performance of Fluorine-18-Fluorodeoxyglucose positron emission tomography in patients with chronic inflammatory bowel disease: a systematic review and a meta-analysis. J Crohns Colitis 7:345–354
39. Treglia G, Alongi P (2014) Inflammatory bowel disease. In: Cistaro A (ed) Atlas of PET/CT in paediatric patients. Springer, Milan, pp 199–200
40. Rypins EB et al (1997) Tc-99m-HMPAO white blood cell scan for diagnosis of acute appendicitis in patients with equivocal clinical presentation. Ann Surg 226(1):58–65
41. Kipper SL (1999) The role of radiolabeled leukocyte imaging in the management of patients with acute appendicitis. Q J Nucl Med 43:83–92
42. Vome M et al (1989) Technetium-99m-HMPAO-labeled leukocytes in detection of inflammatory lesions: comparison with gallium-67-citrate. J Nucl Med 30:1332–1336
43. Lantto EH et al (1991) Fast diagnosis of abdominal infections with technetium-99m-HMPAO-labeled leukocytes. J Nucl Med 32:2029–2034
44. Cucinotta M, Cistaro A (2014) Appendicite. In: Cistaro A (ed) Atlas of PET/CT in paediatric patients. Springer, Berlin/London, p 201
45. Torigian DA (2009) Utility of ^{18}F-FDG-PET/CT imaging in the diagnosis of appendicitis. Hell J Nucl Med 12:281–282
46. Warrington JC, Charron M (2007) Pediatric gastrointestinal nuclear medicine. Semin Nucl Med 37:269–285
47. Heyman S et al (1979) An improved method for the diagnosis of gastroesophageal reflux and aspiration in children (milk scan). Radiology 131:479–482
48. Rudd TG, Christie DL (1979) Demonstration of gastroesophageal reflux in children by radionuclide gastroesophagography. Radiology 131:483–486
49. Blumhagen JD et al (1980) Gastroesophageal reflux in children: radionuclide gastroesophagography. AJR Am J Roentgenol 135:1001–1004
50. Klein HA (1995) Esophageal transit scintigraphy. Semin Nucl Med 25:306–317
51. Urbain JLC (2003) Esophageal transit, gastroesophageal reflux, and gastric emptying. In: Sandler MP, Coleman RE, Patton JA et al (eds) Diagnostic nuclear medicine, 4th edn. Lippincott Williams and Wilkins, Philadelphia, pp 487–501
52. Mann MD, Wynchank S (2004) Esophageal function (transport and motility). In: Ell PJ, Gambhir SS (eds) Nuclear medicine in clinical diagnosis and treatment, 3rd edn. Churchill Livingstone, Edinburgh, pp 789–803
53. Da-Costa-Pinto EAL et al (2004) A functional study of caustic strictures of the esophagus in children. Braz J Med Biol Res 37:1623–1630
54. Zarate N et al (2001) Prospective evaluation of esophageal motor dysfunction in Down's syndrome. Am J Gastroenterol 96:1718–1724
55. Bautista A et al (1996) Motor function of the esophagus after caustic burn. Eur J Pediatr Surg 6:204–207

56. Gainey MA (2000) Radionuclide diagnosis. In: Walker WA, Durie PR, Hamilton JR et al (eds) Pediatric gastrointestinal disease, 3rd edn. B.C. Decker, Hamilton, pp 1655–1675
57. Seibert JJ et al (1983) Gastric emptying in children: unusual patterns detected by scintigraphy. AJR Am J Roentgenol 141:49–51
58. Rosen PR, Treves S (1984) The relationship of gastroesophageal reflux and gastric emptying in infants and children: Concise communication. J Nucl Med 25:571–574
59. Shaffer EA et al (2000) Gallbladder disease. In: Walker WA Durie PR Hamilton JR (ed) Pediatric gastrointestinal disease, 3rd edn. BC Decker Hamilton, Ontario, pp 1291–1311
60. Wessmann HS et al (1979) Rapid and accurate diagnosis of acute cholecystitis with 99mTc-HIDA cholescintigraphy. AJR Am J Roentgenol 132:523–528
61. Chatterton BE (2004) Gastric motility. In: Ell PJ, Gambhir SS (eds) Nuclear medicine in clinical diagnosis and treatment, 3rd edn. Churchill Livingstone, Edinburgh, pp 805–818
62. Avansino JR et al (1999) Characterization and management of paraesophageal hernias in children after antireflux operation. J Pediatr Surg 34:1610–1614
63. Skarsgard PL et al (1998) Balloon pyloroplasty in children with delayed gastric emptying. Can J Surg 41:151–155
64. Kiewiet JJ et al (2012) A systematic review and meta-analysis of diagnostic performance of imaging in acute cholecystitis. Radiology 264:708–720
65. Tulchinsky M et al (2010) SNM practice guideline for hepatobiliary scintigraphy 4.0. J Nucl Med Technol 38:210–218
66. Schwarz SM. Biliary Atresia. Available on url: http://www.emedicine.com/ped/topic237.htm. Accessed on 6th Aug 2014.
67. Treves ST et al (2011) Nuclear medicine in the first year of life. J Nucl Med 52:905–925
68. Spivak W et al (1987) Diagnostic utility of hepatobiliary scintigraphy with 99mTc-DISIDA in neonatal cholestasis. J Pediatr 110:855–861
69. Poddar U et al (2004) Ursodeoxycholic acid-augmented hepatobiliary scintigraphy in the evaluation of neonatal jaundice. J Nucl Med 45:1488–1492
70. De Winter F et al (2002) Promising role of 18F-fluoro-D-deoxyglucose positron emission tomography in clinical infectious diseases. Eur J Clin Microbiol Infect Dis 21: 247–257
71. Sturm E et al (2006) Fluordeoxyglucose positron emission tomography contributes to management of pediatric liver transplantation candidates with fever of unknown origin. Liver Transpl 12:1698–1704
72. Arnoux JB et al (2012) Con-genital hyperinsulinism: current trends in diagnosis and therapy. Orphanet J Rare Dis 6:63
73. Senniappan S et al (2012) Hyperinsulinaemic hypoglycaemia: genetic mechanisms, diagnosis and management. J Inherit Metab Dis 35:589–601
74. Santiago-Ribeiro M et al (2006) Hyperinsulinism of infancy: noninvasive differential diagnosis. In: Charron M (ed) Pediatric PET imaging. Springer, New York, pp 472–485
75. Otonkoski T et al (2006) Noninvasive diagnosis of focal hyperinsulinism of infancy with 18F-DOPA positron emission tomography. Diabetes 55:13–18
76. de Lonlay P et al (2006) Congenital hyperinsulinism: pancreatic [18F]Fluoro-L-dihydroxyphenylalanine (DOPA) positron emission tomography and immunohistochemistry study of DOPA decarboxylase and insulin secretion. J Clin Endocrinol Metab 91:933–940
77. Rufini V, Pizzoferro M (2014) Congenital hyperinsulinism. In: Cistaro A (ed) Atlas of PET/CT in paediatric patients. Springer, Berlin/London, p 249
78. Mohnike W et al (2011) Positron emission tomography/computed tomography diagnostics by means of fluorine-18-L-dihydroxyphenylalanine in congenital hyperinsulinism. Semin Pediatr Surg 20:23–27
79. Hardy OT et al (2007) Accuracy of [18F]fluorodopa positron emission tomography for diagnosing and localizing focal congenital hyperinsulinism. J Clin Endocrinol Metab 92:4706–4711

80. Blomberg BA et al (2013) The value of radiologic interventions and (18)F-DOPA PET in diagnosing and localizing focal congenital hyperinsulinism: systematic review and meta-analysis. Mol Imaging Biol 15:97–105
81. Treglia G et al (2012) Diagnostic performance of fluorine-18-dihydroxyphenylalanine positron emission tomography in diagnosing and localizing the focal form of congenital hyperinsulinism: a meta-analysis. Pediatr Radiol 42:1372–1379
82. Masue M et al (2011) Diagnostic accuracy of [(1)(8)F]-fluoro-L-dihydroxyphenylalanine positron emission tomography scan for persistent congenital hyperinsulinism in Japan. Clin Endocrinol (Oxf) 75:342–346
83. Zani A et al (2011) The predictive value of preoperative fluorine-18-L-3,4-dihydroxyphenylalanine positron emission tomography-computed tomography scans in children with congenital hyperinsulinism of infancy. J Pediatr Surg 46:204–208
84. Proujansky R (1996) Protein losing enteropathy. In: Walker WA, Dun PR, Hamilton JR, Walker-Smith JA, Watkins JB (eds) Pediatric gastrointestinal disease, 2nd edn. Mosby, St. Louis, pp 971–979
85. Gleason WA (1993) Protein-losing enteropathy. In: Wyllie R, Hyams SJ (eds) Pediatric gastrointestinal disease. WB Saunders, Philadelphia, pp 536–543
86. Suzuki C et al (1997) 99mTc-HSA-D scintigraphy in the diagnosis of protein-losing gastroenteropathy due to secondary amyloidosis. J Gastroenterol 32:78–82
87. Divgi CR et al (1986) Technetium-99m serum albumin scintigraphy in the diagnosis of protein-losing enteropathy. J Nucl Med 27:1710–1712
88. Takeda H et al (1991) Protein-losing gastroenteropathy detected by technetium-99m-labeled human serum albumin. Am J Gastroenterol 86:450–453
89. Yoshida T et al (1987) Technetium-99m serum albumin measurement of gastrointestinal protein loss in a subtotal gastrectomy patient with giant hypertrophic gastritis. Clin Nucl Med 12:773–776
90. Hildebrand P et al (1989) Localization of enteral protein loss by 99m-technetium-albumin-scintigraphy. Eur J Nucl Med 15:217–218
91. Purl AS et al (1992) Intestinal lymphangiectasia: evaluation by CT and scintigraphy. Gastrointest Radiol 17:119–121
92. Oommen R et al (1992) Tc-99m albumin scintigraphy in the localization of protein loss in the gut. Clin Nucl Med 17:787–788
93. Lan JA et al (1988) Protein-losing enteropathy detected by 99mTc-labeled human serum albumin abdominal scintigraphy. J Pediatr Gastroenterol Nutr 7:872–876
94. Sano T et al (1991) Massive intestinal albumin loss after Fontan operation. Acta Paediatr Jpn 33:384–388
95. Shields E et al (1996) Visualization of protein-losing enteropathy in infantile systemic hyalinosis with Tc-99m HSA after albumin challenge. Clin Nucl Med 21:415–416
96. Halaby H et al (2000) 99mTc-human serum albumin scans in children with protein-losing enteropathy. J Nucl Med 41:215–219
97. Cook BJ et al (2005) Radionuclear transit to assess sites of delay in large bowel transit in children with chronic idiopathic constipation. J Pediatr Surg 40:478–483
98. Wheatley JM et al (1999) Slow transit constipation in children. J Pediatr Surg 34:829–832
99. Bastisto Casasnovas A et al (1991) Measurement of colonic transit time in children. J Pediatr Gastroenterol Nutr 13:42–45
100. Metcalf AM et al (1987) Simplified assessment of segmental colonic transit. Gastroenterology 92:40–47
101. Weaver LT, Steiner H (1984) The bowel habit of young children. Arch Dis Child 59:649–652
102. Tota G et al (1998) Use of radionuclides in the evaluation of intestinal transit time in children with idiopathic constipation. Pediatr Med Chir 20:63–66
103. Nothgi AL et al (1994) Use of geometric centre and parametric images in scintigraphy colonic transit studies. Gastroenterology 107:1270–1277

104. Hardy JG, Perkins AC (1985) Validity of the geometric mean correction in the quantification of the whole bowel transit. Nucl Med Commun 6:217–224
105. Pasha SF et al (2008) Double-balloon enteroscopy and capsule endoscopy have comparable diagnostic yield in small-bowel disease: a meta-analysis. Clin Gastroenterol Hepatol 6:671–676
106. Mitchell SH et al (2004) A new view of occult and obscure gastrointestinal bleeding. Am Fam Physician 69:875–881
107. Smith R et al (1987) 99mTc RBC scintigraphy: correlation of gastrointestinal bleeding rates with scintigraphic findings. AJR Am J Roentgenol 148:869–874
108. Roy HK, Ozden N (2003) Obscure causes of upper gastrointestinal bleeding. In: Kim KE (ed) Acute gastrointestinal bleeding: diagnosis and treatment. Humana Press, Totowa, pp 111–133
109. Gayle M, Kissoon N (2005) Gastrointestinal bleeding. In: Wolfson AB, Harwood-Nuss A (eds) Harwood-Nuss'; clinical practice of emergency medicine, 4th edn. Lippincott Williams & Wilkins, Philadelphia, pp 1231–1236
110. Aiges HW (1988) Gastrointestinal bleeding. In: Silverberg M, Daum F (eds) Textbook of pediatric gastroenterology, 2nd edn. Year Book Medical Publishers, Chicago, pp 137–148
111. Treves ST, Grand RJ (1995) Gastrointestinal bleeding. In: Treves ST (ed) Pediatric nuclear medicine, 2nd edn. Springer, New York, pp 453–465
112. Maurer AH (2004) Gastrointestinal bleeding. In: Ell PJ, Gambhir SS (eds) Nuclear medicine in clinical diagnosis and treatment, 3rd edn. Churchill Livingstone, Edinburgh, pp 911–917
113. Alavi A et al (2003) Scintigraphic detection and localization of gastrointestinal bleeding sites. In: Sandler MP, Coleman RE, Patton JA et al (eds) Diagnostic nuclear medicine, 4th edn. Lippincott Williams and Wilkins, Philadelphia, pp 531–551
114. Zuckier LS (2003) Acute gastrointestinal bleeding. Semin Nucl Med 33:297–311
115. Herzog CE et al (2000) Childhood cancers: hepatoblastoma. Oncologist 5:445–453
116. Litten JB, Tomlinson GE (2008) Liver tumors in children. Oncologist 13:812–820
117. Zsiros J et al (2010) Successful treatment of childhood high-risk hepatoblastoma with dose-intensive multiagent chemotherapy and surgery: final results of the SIOPEL-3HR study. J Clin Oncol 28:2584–2590
118. Avila LF et al (2006) Liver transplantation for malignant tumours in children. Eur J Pediatr Surg 16:411–414
119. Hertl M, Cosimi AB (2005) Liver transplantation for malignancy. Oncologist 10:269–281
120. King SJ et al (1993) Value of CT in determining the resectability of hepatoblastoma before and after chemotherapy. Am J Roentgenol 160:793–798
121. Iacob D et al (2010) Mixed hepatoblastoma in child. Case report. Med Ultrason 12:157–162
122. Perilongo G et al (2000) SIOPEL trials using preoperative chemotherapy in hepatoblastoma. Lancet Oncol 1:94–100
123. Spieth ME, Kasner DL (2002) A tabulated summary of FDG literature. J Nucl Med 43:441
124. Bar-Shalom R et al (2000) PET imaging in oncology. Semin Nucl Med 30:150–185
125. Hustinx R et al (2002) Whole-body FDG-PET imaging in the management of patients with cancer. Semin Nucl Med 32:35–46
126. Horie A et al (1979) Ultrastructural comparison of hepatoblastoma and hepatocellular carcinoma. Cancer 44:2184–2193
127. Warfel KA, Hull MT (1992) Hepatoblastomas: an ultrastructural and immunohistochemical study. Ultrastruct Pathol 16:451–461
128. Shiojiri N (1981) Enzymo- and immunocytochemical analyses of the differentiation of liver cells in the prenatal mouse. J Embryol Exp Morphol 62:139–152
129. Patel CD, Kumar R (2007) Positron emission tomography and positron emission tomography-computerized tomography in pediatric patients. J Indian Assoc Pediatric Surg 12:120–124
130. Yang WT, Johnson PJ (1999) Monitoring response to treatment in liver tumours. Baillieres Best Pract Res Clin Gastroenterol 13:637–654
131. Figarola MS et al (2005) Recurrent hepatoblastoma with localization by PET-CT. Pediatr Radiol 35:1254–1258

132. Sironi S et al (2004) Recurrent hepatoblastoma in orthotopic transplanted liver: detection with FDG positron emission tomography. Am J Roentgenol 182:1214–1216
133. Wong KKY et al (2004) The use of positron emission tomography in detecting hepatoblastoma recurrence - a cautionary tale. J Pediatr Surg 39:1779–1781
134. Philip I, Shun A et al (2005) Positron emission tomography in recurrent hepatoblastoma. Pediatr Surg Int 21:341–345
135. Mody RJ et al (2006) FDG PET for the study of primary hepatic malignancies in children. Pediatr Blood Cancer 47:51–55
136. Cistaro A et al (2013) A comparison between 18F-FDG PET/CT imaging and biological and radiological findings in restaging of hepatoblastoma patients. Biomed Res Int 2013;2013:709037. Doi 10.1155/2013/709037. Epub 2013 Aug 26